Synthesis and Characterization of Photobase Generators for Pitch Division Photolithography

Presented by Wade Wang

In partial fulfillment of the requirements for graduation with the Dean's Scholars Honors Degree in Biochemistry

Undergraduate Honors Thesis

The University of Texas at Austin

May, 2013

_____ _____

Dr. C. Grant Willson Date
Supervising Professor

_____ _____

Dr. John F. Stanton Date
Honors Advisor

Acknowledgements

This work would not be possible if it was not for all the support and mentorship I received throughout my undergraduate career. I would like to thank Ryan Mesch and Xinyu Gu for allowing me the fortune of working with them and teaching me basic organic chemistry lab techniques when I first started in the group as a freshman. I anticipate my appreciation will only grow as I become a graduate student and understand how important patience is when working with an undergraduate, let alone a freshman. Furthermore, all my colleagues Willson group have been extremely helpful and kind. Such a remarkable group of people has spoiled me; my future graduate school experience will be excellent if I can find a group of people as wonderful as all of you. I thank Kathleen Sparks and Donna Martin for their help on administrative issues. You two have enabled me to focus on the science by keeping paperwork and bureaucracy to a minimal.

Outside the chemistry lab, I'm extremely lukcy to be a member of Dean's Scholars, the natural sciences honors program. I've met many great people through events with other scholars such as Friday lunch, musicale, dinners, etc. My only regret is that I'm unable to spend another year with such fantastic company. Thanks to Bert Xue, Andrew Pansick, Steven Stolte II, and Dr. David Hillis for helping revise and draft my thesis. I thank Dr. Ruth Shear for teaching me how to be a more effective teaching assistant and writing my letters of recommendation, despite being busy with running the freshman research initiative, Beckman scholars program, undergraduate research focus group, etc. I am also indebted to my family and friends, whose encouraging words and camaraderie have carried me to where I am now.

Most importantly, I would like to thank Dr. Willson for being the best research advisor I could ever ask for. Because of him, I was able to discover my passion for organic chemistry and build a foundation for further graduate studies in such a fascinating subject. Lastly, I appreciate the University of Texas at Austin for providing me with an excellent environment for undergraduate studies and an unforgettable undergraduate experience.

Synthesis and Characterization of Photobase Generators for Pitch Division Photolithography

Wade Wang
The University of Texas at Austin

Supervisor: Dr. C. Grant Willson

Pitch division lithography is a resolution enhancing technique that doubles the resolution of features in a photomask when recorded in photoresist without imposing costly additional steps or demanding manufacturing equipment. In conventional chemically amplified photolithography, acid is generated when the photoresist is exposed to ultraviolent radiation. The photogenerated acid then catalyzes chemical reaction that generates a solubility change in the photoresist polymer. Once a sufficient quantity of acid is produced, known as the threshold acid concentration, the resist becomes soluble in a developing solution. A pitch division resist generates acid at medium UV doses, but at high dose, the acid is neutralized. This results in effectively crossing the threshold acid concentration twice, and produces two features instead of one.

Pitch division performance is accomplished by incorporating a photobase generator (PBG) into the resist. The amount of PBG is in excess of the photoacid generator, but the rate of base generation must be less than that of acid generation Pitch division lithography works well with typical photobase generators. However, the line edge roughness of the resulting features is unacceptable for industrial applications. One cause of unsatisfactory line edge roughness is a low chemical contrast at the threshold acid concentration. The acid concentration in a pitch division photoresist does not change as sharply as it does in a conventional resist due to partial quenching of acid in medium dose regions by the photo-generated base. This problem could be remedied by creating a photobase generator that has a built in delay in onset of base production and then accelerates as a function of increasing dose. To achieve this type of higher order kinetics, we propose a two-stage photobase generator that must convert to an active form before generating base. Various novel two-stage photobase generators have been synthesized and are currently

undergoing kinetic and imaging characterization. This thesis will describe the characterization of first generation photobase generators as well as the synthesis and ongoing characterization efforts of second generation photobase generators.

Table of Contents

Chapter 1: Pitch Division Lithography with Photobase Generators

Introduction to Pitch Division and Lithography

Photolithography is the process used by the semiconductor industry to generate patterns on silicon wafers and thereby produce logic devices, memory, hard disk drives, etc. First, a silicon wafer is coated with a thin film of photoresist. The purpose of the photoresist is two-fold: the photoresist must respond to light (photo-) as well as shield the silicon wafer from later processing steps such as reactive ion etching or ion implantation (-resist). In order to achieve both these effects, the photoresist is comprised of an etch resistant polymer as well as a photoresponsive molecule. Light shines through a mask and selectively exposes certain areas of the film. After exposure and development, the resist in the areas exposed to light can be selectively removed. Those areas are no longer protected by the resist and can be manipulated without modifying the unexposed areas, which are still protected by the resist to enable pattern transfer into the substrate material. Photolithography has worked well for the industry in the past to manufacture devices. However, there is a constant impetus to advance lithography technology in order to perpetuate improvements in productivity and technology, and the resolution for photolithography, the most common method of wafer patterning in the semiconductor industry, is currently limited at about 36 nm by physical barriers. These barriers are wavelength (λ), numerical aperture (NA), and the process latitude factor (k_1) (Fig. 1.1).

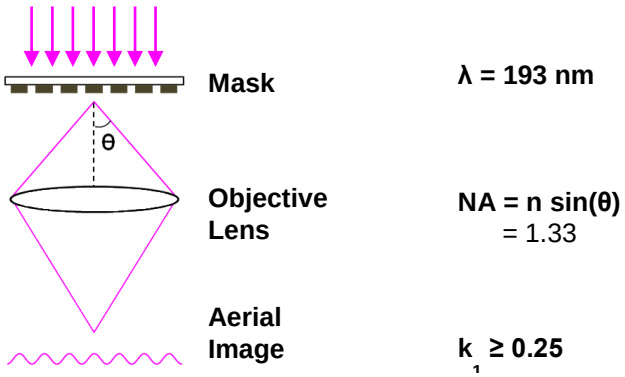

$$Resolution = k_1 \frac{\lambda}{\mathrm{NA}} = 36\ \mathrm{nm}$$

Figure 1.1. Physical barriers of photolithography and current resolution limit

This has led the exploration of new technologies for patterning of sub-30 nm half pitch features. One such technique that shows promise is multiple patterning lithography (MPL). MPL will allow the fabrication of sub-30 nm features on current photolithographic equipment. One MPL technique is double patterning lithography. However, this technique requires the use of additional masks. Moreover, multiple steps must be added to the manufacturing process for each mask, each of which increases cost and decreases yield. A pitch division photoresist, on the other hand, can achieve results comparable to MPL without the implementation of additional masks and manufacturing steps, thus reducing fabrication cost and increasing tool throughput. Consider a conventional chemically amplified photoresist: a photoacid generator (PAG) generates acid according to a rate constant when the photoresist is exposed to ultraviolent radiation (Fig. 1.2). The photogenerated acid then catalyzes the deprotection of t-butoxycarbonyl groups on the photoresist polymer when heat is applied, which makes the polymer soluble in basic developer (Fig. 1.3). Once a sufficient percentage of the polymer is deprotected, the resist becomes soluble in the developing solution. The acid concentration when this occurs is referred to as the threshold acid concentration. After development, the exposed silicon can be etched or otherwise processed without effecting the rest of the silicon wafer.[1]

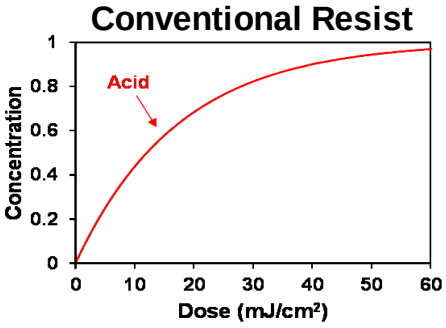

$$PAG + h\nu \xrightarrow{k_a} Acid$$

$$[Acid] = [PAG]_0(1 - e^{-k_a * Dose})$$

Figure 1.2. Acid generation curve of a generic PAG with an acid generation constant of $k_a = 8.87 \times 10^{-2}$ cm^2/mJ.

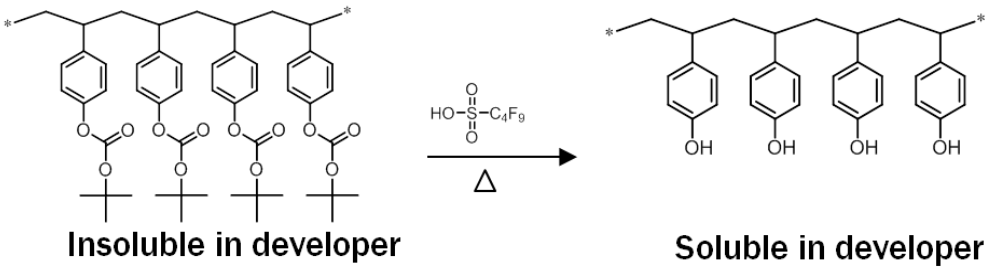

Figure 1.3. A photoresist polymer chemistry in the presence of acid and heat

The pitch division resist formulation is designed to generate acid at low to medium doses much like a traditional resist. However, unlike a traditional resist, it neutralizes the acid at higher doses. The production and subsequent neutralization of the acid means the net concentration of acid crosses the acid threshold concentration twice, resulting in two features instead of one. In order to achieve this effect, a photobase generator (PBG) can be used to generate base to neutralize the acid before the photoresist polymer is deprotected. The rate of base generation (k_b) must be slower than the rate of acid generation (k_a), and the loading of PBG must be greater than PAG (Fig. 1.4). In sum, pitch division resists can produce double the number of features of conventional resists through changes in the photoresist chemistry (Fig. 1.5).[2]

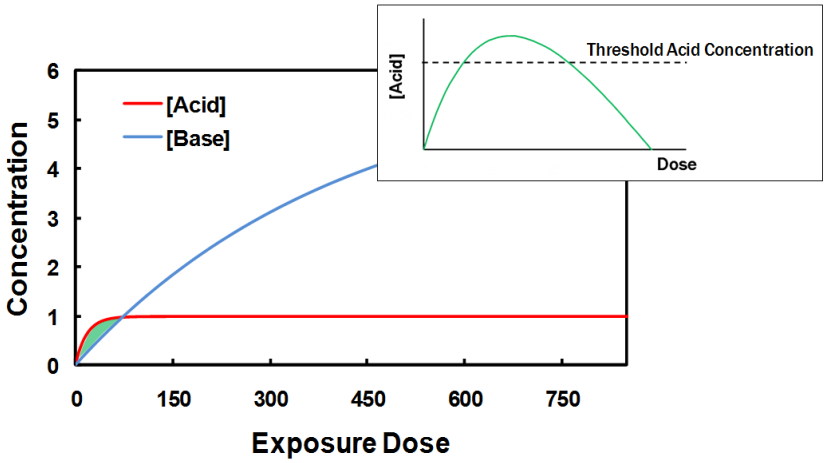

Figure 1.4. Theoretical acid, base, and net acid curves for a dual tone resist

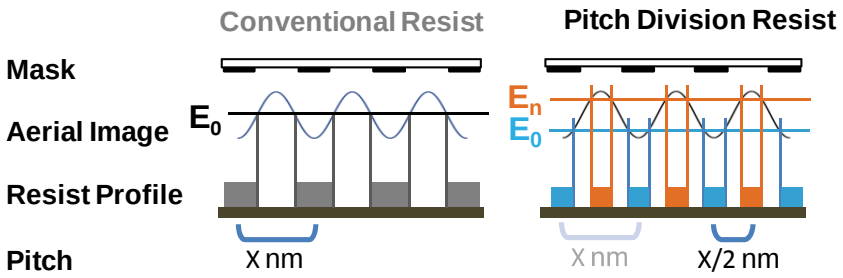

Figure 1.5. A conventional resist vs. a PD resist

Evaluation of PBG Kinetics

Three different types of PBGs were tested: benzoin carbamates, *o*-nitro benzyl carbamates, and sulfonamides. Each type of PBG has a different absorbance and quantum yield, and consequently each decomposes at different rate upon irradiation of UV light[3-5]. Thus, each PBG has a different base generation constant, k_b. The potential for PBG use in PD lithography can be assessed by comparing the experimentally determined k_b to the k_a of a commonly used PAG, triphenylsulfonium trifluoromethanesulfonate (TPS-Tf). For PD to work, the k_b must be less than the k_a(TPS-Tf: $k_a = 8.87 \times 10^{-2}$ cm^2/mJ).

The PBGs 2-nitrobenzyl cyclohexylcarbamate (CHA-CARB), 1,2-bis(3,5-dimethoxyphenyl)-2-oxoethyl cyclohexylcarbamate (Tetramethoxybenzoin Cyclohexylcarbamate), and N-heptyl-4-methylbenzenesulfonamide (SF3) were synthesized by former group members (Fig 1.6).

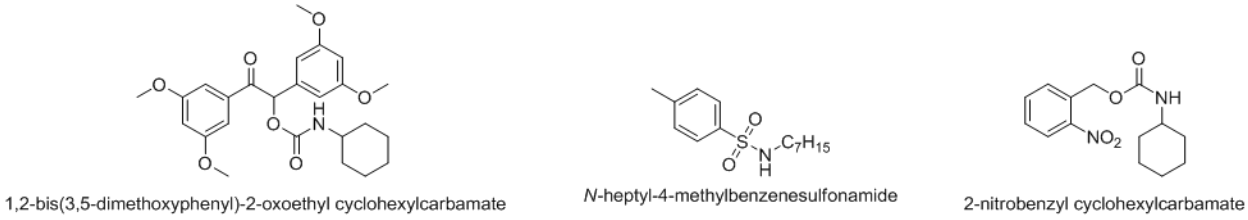

Figure 1.6. Provided PBGs to be tested

The PBG 2-nitrobenzyl dicyclohexylcarbamate (DCHA-CARB) was synthesized through two nucleophilic acyl substitution reactions (Fig. 1.7).

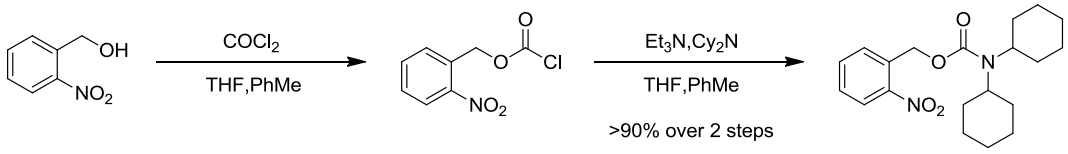

Figure 1.7. Synthesis route of 2-nitrobenzyl dicyclohexylcarbamate

Each of the PBGs was dissolved in acetonitrile and the solutions were purged with nitrogen gas for 5 minutes prior to exposure. Each solution was exposed to increments of 248 nm deep UV (DUV) radiation and conversion was assessed by UV-Vis spectroscopy. The DUV exposure dosage was carefully calibrated using a surface fit model of laser energy vs. position (Fig. 1.8) and integrated over the area of the cuvette.

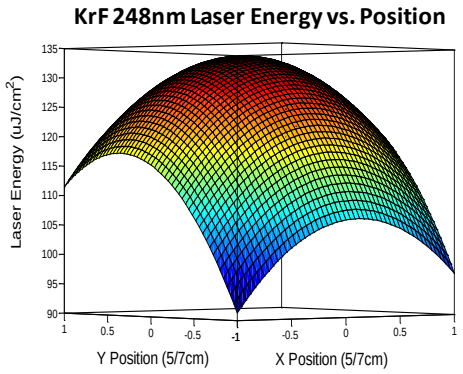

Figure 1.8. Surface plot of 248 nm laser energy vs. position

The dose was then corrected for the distance from the source and the absorption of the solution and cuvette. The Beer-Lambert law was used as a basis for calculating the dose. (Equation 1.9).

$$A = -\log_{10}\left(\frac{I}{I_0}\right)$$

Equation 1.9. The Beer-Lambert law relating intensity and absorbance. In this case, "I" represents the intensity at a given slice. "I_0" represents the intensity at the surface of the solution

The intensity at the surface of the solution, I_0, can be determined by accounting for the loss of laser energy due to distance and conical divergence of the beam, $(d/d+z)^2$, and transmission of

the cuvette wall, TCW. If the extinction coefficient of the solution is known (Equation. 1.10), which can be measured by UV-Vis, the intensity of the laser at a certain position, z, can be calculated by solving the Beer-Lambert relation for I. Dose is calculated by integrating this intensity value over the thickness of the solution and the total number of pulses, TP. This is essentially summing all the laser intensity values over the entire solution. Integrating over the thickness of the solution, z, will account for the loss of laser energy due to light diverging as the slice gets further away from the laser source. Integrating over the total number of pulses accounts for the absorbance change of the solution as the PBG is converted to products (Equation 1.11 & Fig. 1.12).

$$Abs = \sum_{n=0}^{\infty} Z_n * Abs \qquad 1 = \sum_{n=0}^{\infty} Z_n$$

Equation 1.10. The absorbance of a solution can be represented by the summation of the absorbance of many small slices of the solution

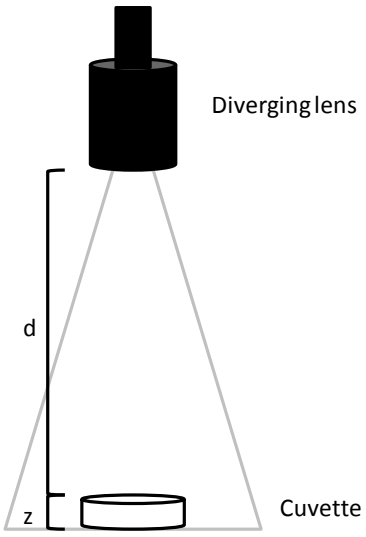

$$Abs(P) * z = -log_{10}\left(\frac{I}{\left(\frac{d}{d+z}\right)^2 * LE * TCW}\right)$$

Solve for I and integrate over specified parameters...

$$Dose = \int_0^1 \int_0^{TP} \frac{TCW * d^2 * LE}{e^{Abs(P)*z*ln(10)} * (d + z)^2} \, dP \, dz$$

Figure 1.11 & Equation 1.12. Determination of dosage. z, distance from top slice to slice of interest. abs, absorption of solution as a function of laser pulses. d, distance from source to top slice. LE, calculated laser energy. TCW, transmission of a single cuvette wall. I, intensity at slice of interest. P, pulses. TP, total pulses.

The percent conversion is then calculated from the UV-Vis data by a fit to the base generation curve (Equation 1.13).

$$[Base] = (1 - e^{-k_b * Dose})$$

Equation 1.13. Base generation curve fitting equation

PBG Kinetic Results

2-Nitrobenzyl cyclohexylcarbamate (CHA-CARB)

CHA-CARB was dissolved in acetonitrile to form a 0.198 mM solution. The solution was then purged with N_2 and exposed to a total of 4.5 mJ/cm^2 of DUV in several dose increments. The percent conversion was assessed by the absorbance at the wavelength of 234 nm. Fitting to the base generation curve showed a k_b of 8.1 x 10^{-4} cm^2/mJ (Fig. 1.14).

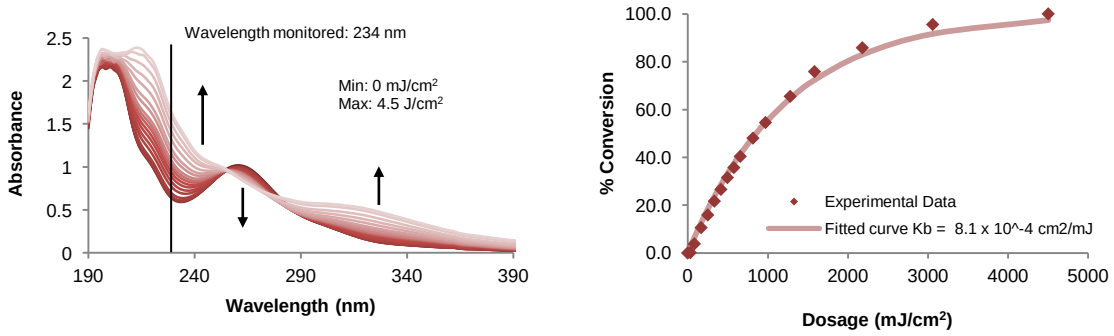

Fig. 1.14. Absorbance and percent conversion data for CHA-CARB

2-Nitrobenzyl dicyclohexylcarbamate (DCHA-CARB)

DCHA-CARB was dissolved in acetonitrile to form a 0.201 mM solution. The solution was then purged with N_2 and exposed to a total of 4.9 J/cm^2 of DUV in many dose increments. The percent conversion was assessed by the absorbance at the wavelength of 234 nm. Fitting to the base generation curve showed a k_b of 8.8 x 10^{-4} cm^2/mJ (Fig. 1.15).

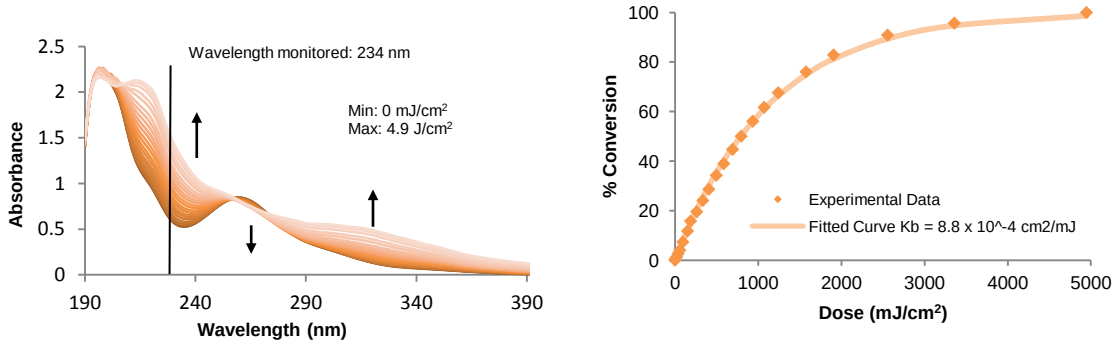

Fig. 1.15. Absorbance and percent conversion data for DCHA-CARB

N-heptyl-4-methylbenzenesulfonamide (SF3)

SF3 was dissolved in acetonitrile to form a 5.9 x 10^{-2} mM solution. The solution was then purged with N_2 and exposed to a total of 7.9 J/cm^2 of DUV in many dose increments. The percent conversion was assessed by the absorbance at wavelength of 260 nm. Fitting to the base generation curve showed a k_b of 7.4 x 10^{-4} cm^2/mJ (Fig. 1.16).

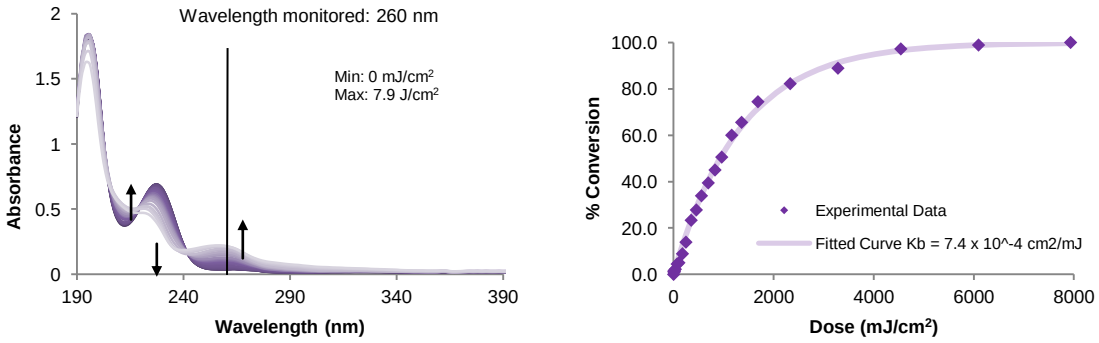

Fig. 1.16. Absorbance and percent conversion data for SF3

1,2-Bis(3,5-dimethoxyphenyl)-2-oxoethyl cyclohexylcarbamate (Tetramethoxybenzoin cyclohexylcarbamate)

Tetramethoxybenzoin cyclohexylcarbamate was dissolved in acetonitrile to form a 4.4 x 10^{-2} mM solution. The solution was then purged with N_2 and exposed to a total of 2.0 J/cm^2 of DUV in many dose increments. The percent conversion was assessed by the absorbance at the wavelength of 300 nm. Fitting to the base generation curve showed a k_b of 3.3x10^{-3} cm^2/mJ (Fig. 1.17).

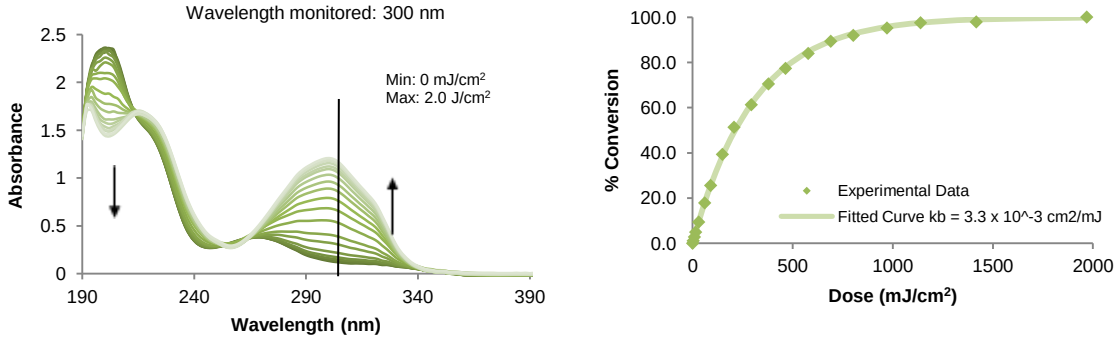

Fig. 1.17. Absorbance and percent conversion data for tetramethoxybenzoin cyclohexylcarbamate

Summary

Compared to the PAG, triphenylsulfonium trifluoromethanesulfonate (k_a = 8.87x10^{-2} cm^2/mJ), all the PBGs tested had a k_b values of less than the k_a of TPS-Tf (Table 1.18). This demonstrates that with the appropriate formulation, these four PBGs could potentially work for PD lithography at 248nm.

PBG	k_b
CHA-CARB	8.1 x 10^{-4} cm^2/mJ
DCHA-CARB	8.8 x 10^{-4} cm^2/mJ
SF3	7.4 x 10^{-4} cm^2/mJ
Tetramethoxybenzoin cyclohexyl carbamate	3.3 x 10^{-3} cm^2/mJ

Table 1.18. Table of PBG k_b values compared to TPS-Tf k_a value

References

(1) Fréchet, J.M.J.; Ito, H.; Willson, C.G. *Proc. Microcircuit Eng.* **260** (1982).

(2) Gu, X.; Bates, C.; Cho, Y.; Costner, E.; Marzuka, F.; Nagai, T.; Ogata, T.; Shi, C.; Sundaresan, A.K.; Turro, N.J.; Bristol, R.; Zimmerman, P.; Willson, C. G. *J. Photopoly. Sci. & Tech.* **22**, 773-781 (2009).

(3) Cameron, J.F.; Fréchet, J.M.J. *J. Am. Chem. Soc.*, **1991**, 4303-4313.

(4) Kutal, C. *Coordination Chem. Reviews*. **2001**, 211, 353–368.

(5) Suyama, K.; Shirai, M. *Prog. Polym. Sci.* **2009**, 34, 194–209.

Chapter 2: Second Generation Photobase Generators

Motivation for a Second Generation

The principle of pitch division works extremely well, but the line edge roughness needs to be improved before pitch division can be used in commercial applications (Fig. 2.1). One cause of poor line edge roughness may be a low chemical contrast at the threshold acid concentration, especially at high doses. This is caused by partial quenching of the acid in medium dose regions by the photo-generated base. The solution to this problem is to incorporate a PBG that more closely follows second order reaction kinetics (Fig. 2.2). Hence, a second generation PBG was sought that incorporates a built-in delay in onset of base production and then accelerates as a function of increasing dose.[3]

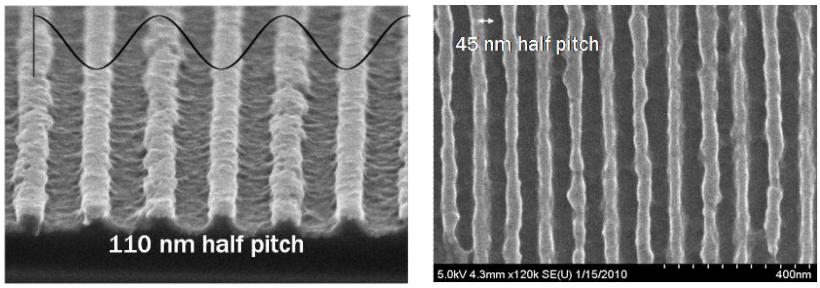

Figure 2.1. Scanning electron microscope images of gratings produced by pitch division.

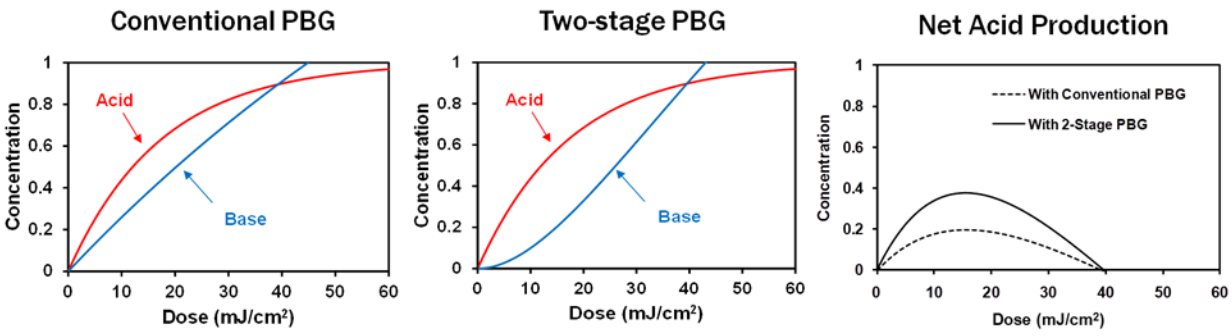

Figure 2.2. Comparison of kinetics for a conventional PBG vs. a two-stage PBG.

Second Generation PBG Design and Synthesis

A known PBG can be modified into a second generation two stage PBG through two methods. The first involves masking the chromophore of the photolabile protecting group in a PBG with another photolabile protecting group. The other method masks the amine base with an additional photolabile protecting group, resulting in two protecting groups directly masking the base. Simulations done by the Willson group have indicated that the kinetics of photolysis for both stages in a two-stage photobase generator should be equivalent to best emulate second order reaction kinetics and achieve the greatest degree of latency. A difunctional PBG can satisfy these requirements by protecting the amine base with the same photolabile protecting group twice (Fig. 2.3). Based on data from previous kinetic and imaging studies, the bis(2-nitrobenzylcarboxy)cyclohexylamine PBG is one ideal candidate for a two-stage PBG.

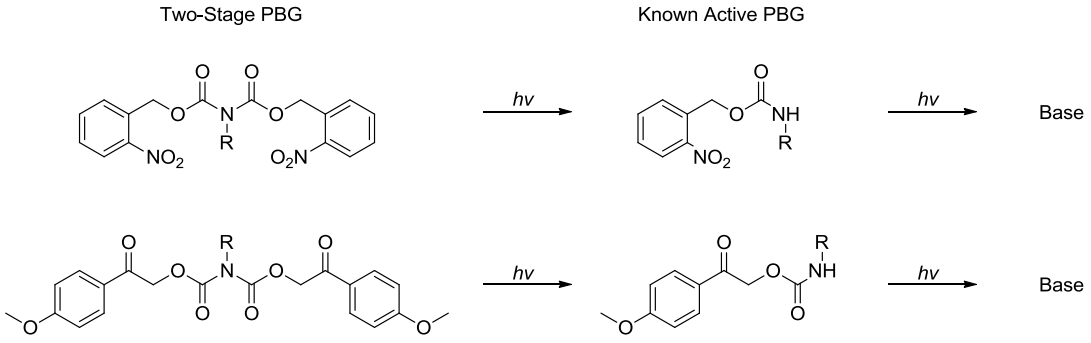

Figure 2.3. Examples of difunctional, two-stage PBGs

The difunctional PBG, bis(2-nitrobenzylcarboxy)cyclohexylamine, was initially synthesized in three steps on a 3.6 mmol scale in a 5% overall yield (Fig 2.4). The first hypothesis for the cause of the low yield was aggregation of the base, potassium bis(trimethylsilyl)amide, in solution.[4] To test this hypothesis, a thorough solvent screen was performed with combinations of solvents that are commonly used with metal amide bases. Different bases were also auditioned for the reaction (Fig. 2.5).[5,6] However, all of the reaction conditions tested failed to produce the desired product.

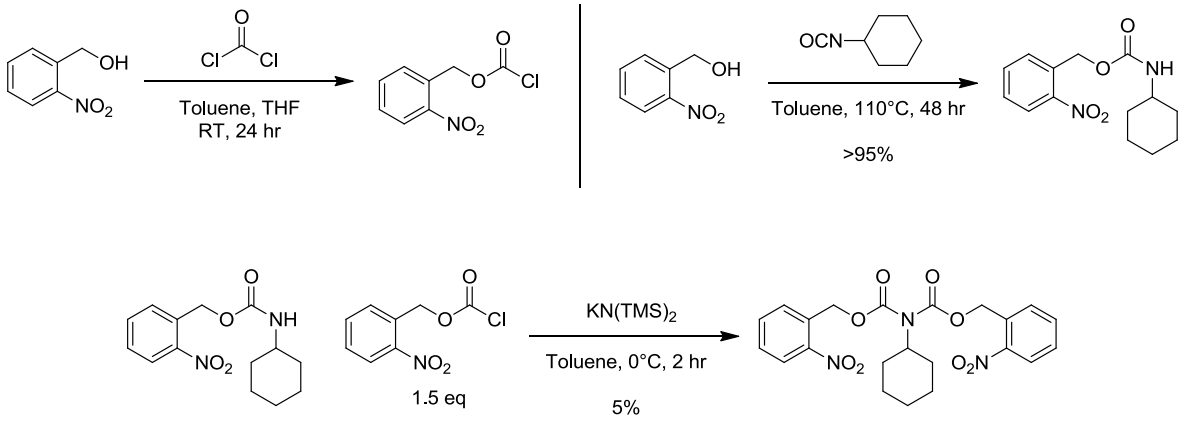

Figure 2.4. Synthetic route for the difunctional o-nitrobenzyl cyclohexylcarbamate PBG

Solvent	Additive	Base	Yield
Toluene		KHMDS	**5%**
THF	HMPA	KHMDS	**NR**
Toluene	THF	KHMSD	**NR**
DCM		KHMDS	**NR**
Toluene	HMPA	KHMDS	**NR**
THF	DMAP	TEA	**NR**
HMPA		KHMDS	**NR**
Pyridine		TEA	**NR**
DMF		KHMDS	**NR**

Figure 2.5. Table of attempted conditions. NR, no reaction

The next hypothesis was inhibition of nucleophile formation by competitive formation of a resonance stabilized benzylic carbanion through deprotonation of the fairly acidic benzyl proton (Fig. 2.6). To test this hypothesis, a reaction was set up with the standard procedure: the carbamate was equilibrated with base and then added dropwise to the electrophile. In the test reaction, the starting carbamate was changed to 4-*tert*-butyl-benzyl cyclohexylcarbamate. Because the *tert*-butyl group on the aromatic ring is not electron withdrawing, the benzylic protons should be significantly less acidic. The test reaction produced the expected product in 50% yield (NMR) after flash chromatography. A control reaction with 2-nitrobenzyl

cyclohexylcarbamate and 4-*tert*-butyl-benzyl chlorocarbonate did not have an improved yield (Fig. 2.7).

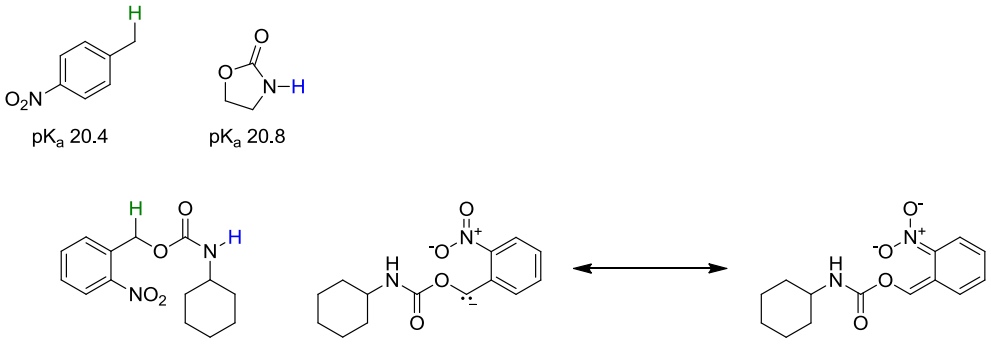

Figure 2.6. Proposed resonance stabilized anion

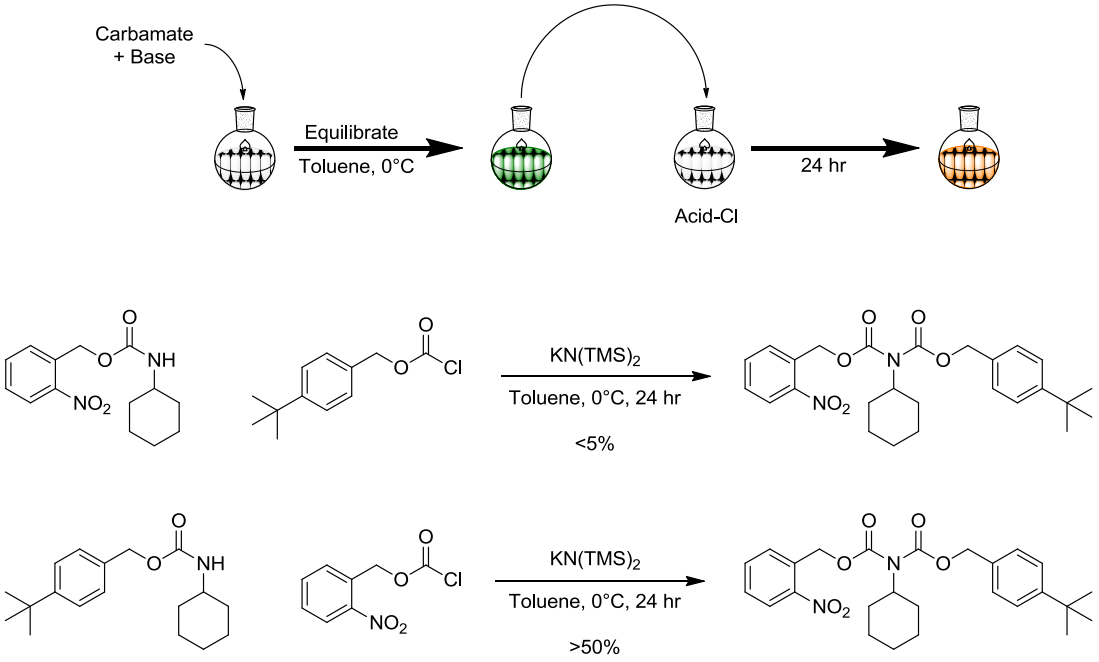

Figure 2.7. The experiments to prove the hypothesis of competitive deprotonation

To confirm that the improved yield was the result of the electronic effects of the nitro group rather than the steric effects of the change of substitution position on the aromatic ring from ortho to para, a reaction was done using 4-nitrobenzyl chloroformate and 4-nitrobenzyl cyclohexylcarbamate. As expected, the reaction did not yield the predicted product. These two

experiments demonstrate that the low yield is a result of the electronic, rather than steric, effects of the nitro group in the ortho position (Fig. 2.8). The yield was ultimately improved to 17% by scaling up the reaction from 3.6 mmol to 40 mmol. The PBG that was synthesized has been sent to collaborators in Japan and is currently undergoing imaging studies.

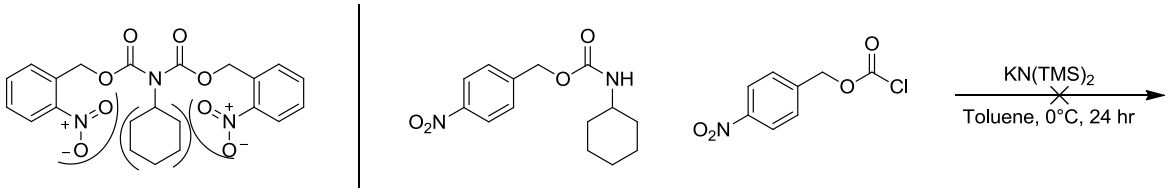

Figure 2.8. The experiment to confirm electronic effects and rule out steric effects

The kinetics of the bis(2-nitrobenzylcarboxy)cyclohexylamine two-stage PBG were studied by ion chromatography. However, preliminary results showed significantly less base generation than expected, potentially due to reactions between the amine and the nitrosobenzaldehyde photoproduct, which then undergoes ring closure to from an indazolone (Fig. 2.9).[7-9] One approach to circumvent this problem was to synthesize an analog of the PBG that disfavors the formation of the transition state to ring closure. Based on the literature, methylating the PBG in the benzyl position will prevent an elimination involved in the ring closure mechanism, but more importantly, the methyl group will hinder nucleophilic attack on the carbonyl carbon.[7-9] Though the benzyl methylated analog will have different kinetics of photolysis due to the slight electron donating properties of the methyl substituent at the benzyl position, it will still exhibit pseudo second order kinetics when exposed to UV radiation. A comparison between bis(1-(2-nitrophenyl)ethylcarboxy)cyclohexylamine and its one stage counterpart can verify the kinetic behavior of a two-stage PBG versus a one stage PBG (Fig. 2.10).

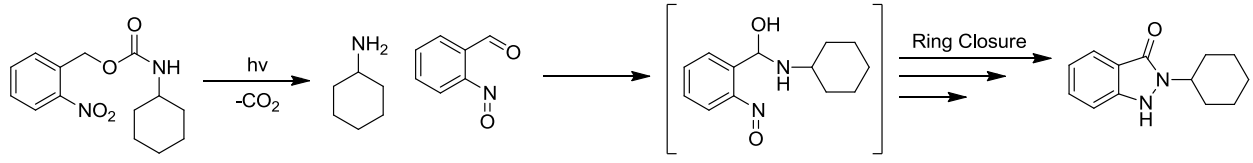

Figure 2.9. Photolysis and subsequent reactions of 2-nitrobenzyl cyclohexylcarbamate[7-9]

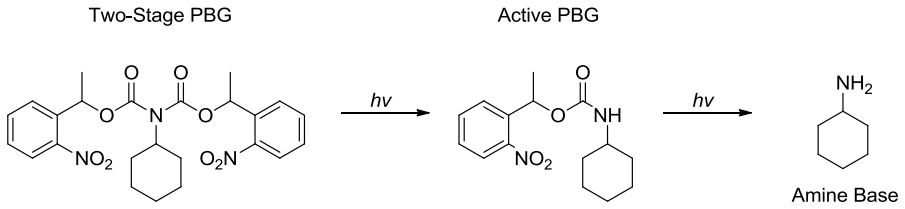

Figure 2.10. New PBG target with the benzyl methylated 2-nitrobenzyl alcohol as the photoactive moiety

Initial efforts to synthesize the benzyl methylated analog of the difunctional o-nitrobenzyl PBG by similar routes were unsuccessful, resulting in a symmetrical carbonate instead of the difunctional carbamate (Fig. 2.11).

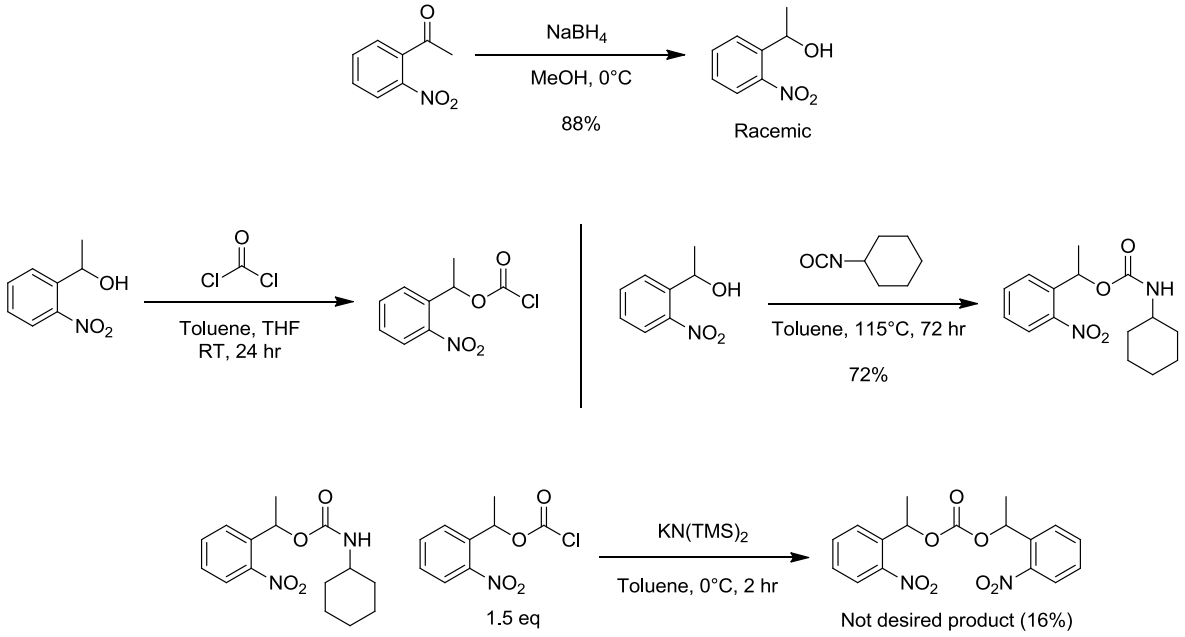

Figure 2.11. Initial attempts to synthesize the benzyl methylated PBG analog, bis(1-(2-nitrophenyl)ethylcarboxy)cyclohexylamine

Two other synthetic routes were designed that avoided the use of strong base with the 2-nitrobenzyl moiety. The bis(carboxy)amine structure was created using a similar synthetic route, but the photoactive functionality was added later through a transition metal catalyzed transcarbamoylation reaction with molecular sieves to absorb ethanol, thereby driving the

equilibrium towards the product (Fig. 2.12). This approach was effective and enabled synthesis of the cyclohexylamine analog of the benzyl methylated second generation PBG.

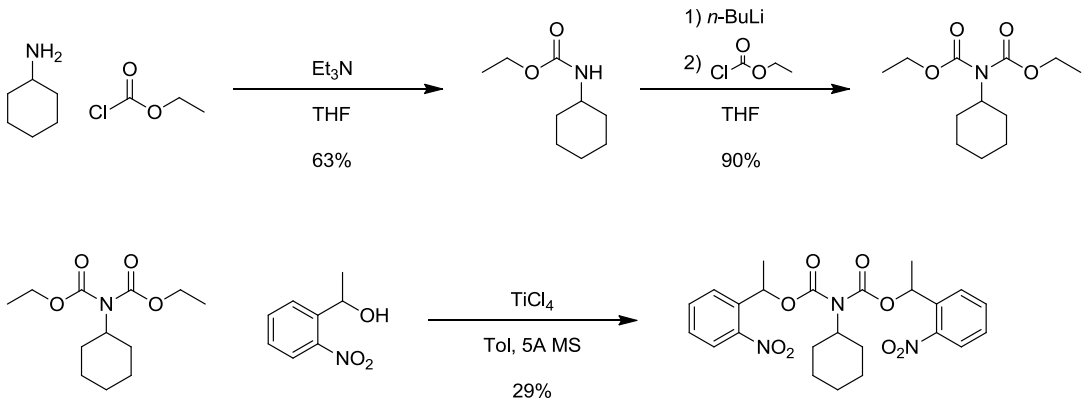

Figure 2.12. Synthetic route to the methylated PBG analog, bis(1-(2-nitrophenyl)ethylcarboxy)cyclohexylamine, by transcarbamoylation

To further slow the rate of side reactions after photolysis of the difunctional two stage PBG, aniline, a less nucleophilic amine base, was substituted for cyclohexylamine. However, the electron withdrawing properties of the aromatic ring resulted in an undesirable side reaction in the transcarbamoylation reaction (Fig. 2.13). However, the modified benzyl methylated two-stage PGB that generates an aniline base was eventually synthesized (Fig. 2.14) and characterized (Fig. 2.15) with the help from my mentor, Ryan Mesch. Andrew Dick played an important role in characterizing the new material by HPLC studies. The second generation, two-stage PBG clearly demonstrates the designed delay in base generation at low dose regions (Fig. 2.15) and it functions effectively in the resist formulation (Fig. 2.16).

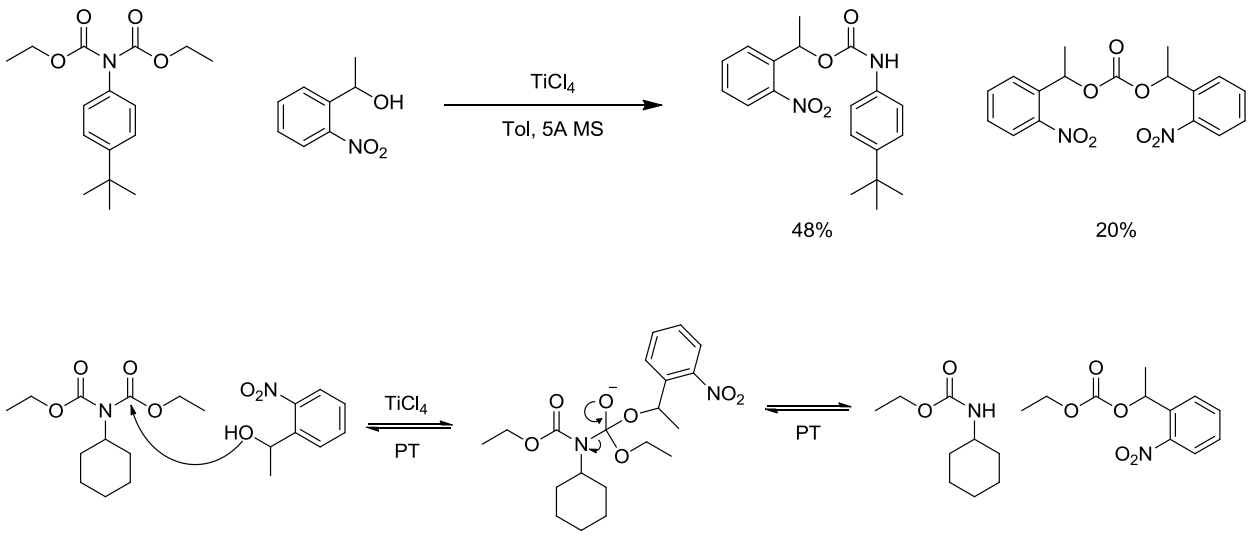

Figure 2.13. The mechanism of the transcarbamoylation side reaction

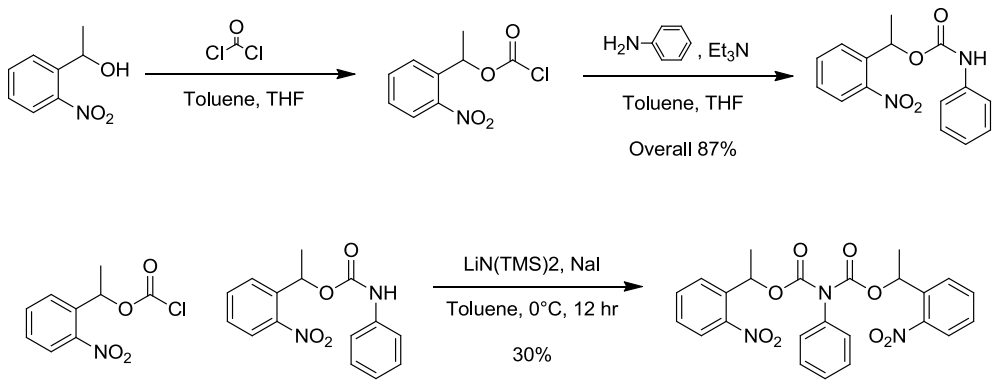

Figure 2.14. The synthetic route to the benzyl methylated two-stage PGB generating an aniline base

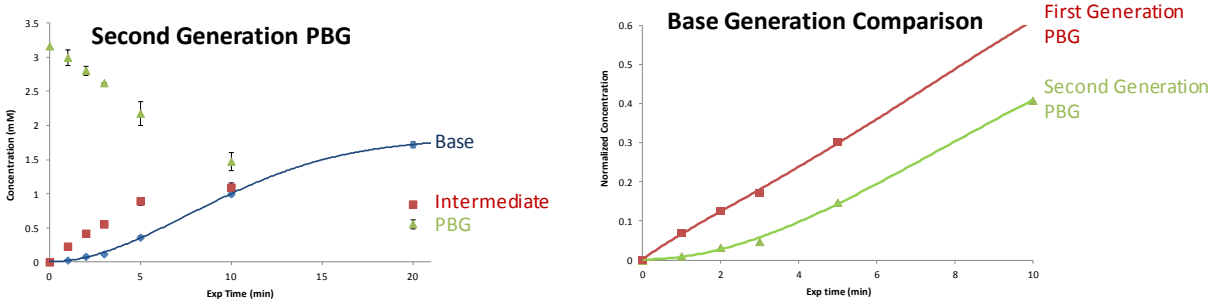

Figure 2.15. HPLC studies of the photolysis of the second generation PBG and a comparison of base generation between the first and second generation PBGs

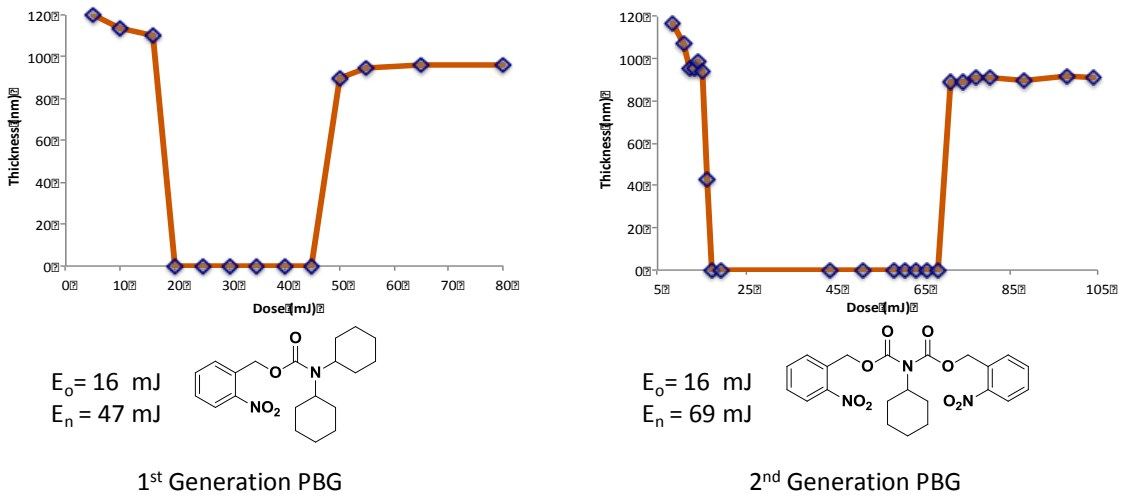

Figure 2.16. A demonstration of pitch division by a first generation and second generation PBG. A silicon wafer was spin coated with photoresist and different areas of the wafer were exposed to incremental amounts of deep UV (excimer laser) radiation. Afterwards, the wafer was heated, allowed to cool, and developed in basic developer. Finally, the film thickness at each exposed area was measured by ellipsometry to correlate dose with film thickness in order to determine E_0, the positive response threshold dose, and E_n, the negative response threshold response dose. Note the negative response threshold appears at a higher dose in the second generation PBG compared to the first generation PBG, indicating a delay in the onset of base generation.

Summary

Multiple synthetic routes to second generation PBGs have been explored. Two target second generation PBGs have been synthesized by the routes and characterized. These PBGs clearly demonstrate latent base generation, as designed. Current work is focused on imaging the second generation PBGs using commercial tools to produce gratings and determining line edge roughness. Line edge roughness is expected to improve.

References

(1) Fréchet, J.M.J.; Ito, H.; Willson, C.G. *Proc. Microcircuit Eng.* **260** (1982).

(2) Gu, X.; Bates, C.; Cho, Y.; Costner, E.; Marzuka, F.; Nagai, T.; Ogata, T.; Shi, C.; Sundaresan, A.K.; Turro, N.J.; Bristol, R.; Zimmerman, P.; Willson, C. G. *J. Photopoly. Sci. & Tech.* **2009**, 22, 773-781.

(3) Gu, X.; Cho, Y.; Kawakami, T.; Hagiwara, Y.; Rawlings, B.; Mesch, R.; Ogata, T.; Kim, T.; Seshimo, T.; Wang, W.; Sundaresan, A.K.; Turro, N.J.; Gronheid, R.; Blackwell, J.; Bristol, R.; Willson, C. G. *Proc. SPIE*. **2011**, 7972.

(4) Tesh, K.F.; Hanusa, T.P.; Huffman, J.C. *Inorg. Chem*. **1990**, 29, 1584-1586.

(5) Wu, Y.C.; Liron, M.; Zhu, J. *J. Am. Chem. Soc.* **2008**, 130, 7148-7152.

(6) Tian, H.; Xuegong, S.; Hongwu, Y.; Lianhe, S.; Yian, S. *J. Org. Chem.* **2002**, 67, 2435-2446.

(7) Yoo, C.L.; Fettinger, J.C.; Kurth, M.J. *J. Org. Chem.* **2005**, 70, 6941-6943.

(8) Kurth, J.M.; Olmstead, M.M.; Haddadin, M.J. *J. Org. Chem.* **2005**, 70, 1060-1062.

(9) Aran, V.J.; Diez-Barra, E.; Hoz, A.; Sanchez-Verdu, P. *Heterocycles*. **1997**, 45, 129.

(10) Patil, R.D.; Joshi, G.; Adimurthy, S. *Ind. Eng. Chem. Res.* **2010**, 49, 8100.

Representative Procedures

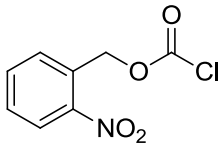

2-nitrobenzyl chloroformate

To a cooled (0 °C) solution of triphosgene (23.505 g, 79.2 mmol) in dry toluene (125 mL) was added dropwise 2-nitrobenzyl alcohol (495 mL of a 1.6 M in THF, 79.2 mmol) over 40 minutes . The reaction was then stirred at RT for 4.5 hours (TLC). After completion of the reaction, the solvents were removed *in vacuo* and gave the product as a light green oil which was used without further purification. TLC R_f 0.86 (DCM); ^{1}H NMR ($CDCl_3$, 400 MHz) δ 8.20 (d, *J* = 8.2 Hz, 1H), 7.66 (m, *J* = 32.3, 14.9, 7.4 Hz, 3H), 5.76 (s, 2H).

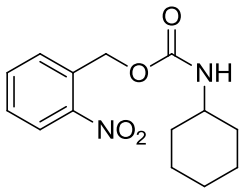

2-nitrobenzyl cyclohexylcarbamate

To a solution of 2-nitrobenzyl alcohol (7.47 g, 48.78 mmol) in dry toluene (200 mL) was added neat cyclohexyl isocyanate (6.85 mL, 53.66 mmol). After stirring under reflux for 48 hours (TLC), the solvent was removed *in vacuo* and replaced with Et_2O. The solution was washed twice with water, rinsed with brine, and dried over Na_2SO_4. Removal of Et_2O *in vacuo* afforded white-yellow solid as product (13.46 g, 48.4 mmol, 99%). TLC R_f 0.51 (30% EtOAc/Hexanes); ^{1}H NMR (400 MHz, $CDCl_3$) δ 8.08 (dd, *J* = 8.2, 1.1 Hz, 1H), 7.69 – 7.54 (m, 2H), 7.46 (t, *J* = 7.6 Hz, 1H), 5.49 (s, 2H), 4.73 (s, 1H), 3.49 (s, 1H), 2.02 – 1.03 (m, 10H); ^{13}C NMR (101 MHz, $CDCl_3$) δ 154.88, 147.45, 133.63, 133.34, 128.85, 128.46, 124.91, 62.99, 50.03, 33.35, 25.42, 24.76; HRMS (ESI): Exact mass calcd for $C_{14}H_{18}N_2NaO_4$ $[M+Na]^+$: 301.11588. Found: 301.11634. M.p. 104 °C - 106 °C

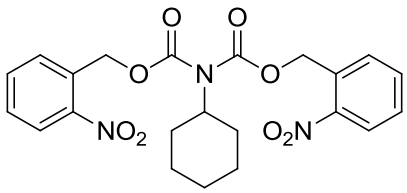

Bis(2-nitrobenzylcarboxy)cyclohexylamine

To a cooled (0 °C) solution of 2-nitrobenzyl cyclohexylcarbamate (11.02 g, 39.6 mmol) in dry toluene (475 mL) was added dropwise $KN(TMS)_2$ (83.2 mL of a 0.5 M in toluene, 41.6 mmol) over 23 minutes. After stirring for 10 minutes, 2-nitrobenzyl chloroformate (198 mL of a 4 M in toluene, 79.2 mmol) was added dropwise over 33 minutes. The reaction was then allowed to warmed to RT and stirred for 14 hours (TLC), concentrated *in vacuo*, and ran through a short plug of silica (DCM). Further purification by flash column chromatography (50% DCM/toluene) and recrystallization ($MeOH/H_2O$ then EtOAc/Hexanes) yielded white solid as product (3.08 g, 17%). TLC R_f 0.69 (DCM); ^1H NMR (400 MHz, $CDCl_3$) δ 8.11 (d, *J* = 8.1 Hz, 2H), 7.63 (dt, *J* = 14.8, 7.3 Hz, 4H), 7.49 (t, *J* = 7.6 Hz, 2H), 5.66 (s, 4H), 4.14 (tt, *J* = 11.6, 3.4 Hz, 1H), 2.01 – 1.58 (m, 7H), 1.21 (dq, *J* = 80.2, 13.2 Hz, 3H); ^{13}C NMR (101 MHz, $CDCl_3$) δ 153.49, 147.30, 133.89, 131.70, 129.09, 128.91, 125.09, 65.37, 58.74, 30.17, 26.20, 25.13; HRMS (ESI): Exact mass calcd for $C_{22}H_{23}N_3NaO_8$ $[M+Na]^+$: 480.13774. Found: 480.13819. M.p. 103 °C - 105 °C

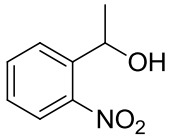

2-nitrophenyl ethanol

To a cooled (0 °C) solution of 1-(2-nitrophenyl)ethanone (100.0 g, 605.5 mmol) in methanol (500 mL) was slowly added sodium borohydride (68.7 g, 1,817 mmol) in small portions over 35 minutes. The reaction was then allowed to warm to RT and stirred for 3 hours (TLC). Afterwards, the reaction was cooled to 0 °C and carefully quenched with water followed by 1 M HCl. The reaction mixture was concentrated *in vacuo* and resuspended in 1 L of Et_2O. The solution was washed with 3 M HCl, saturated $NaHCO_3$, rinsed with brine, and dried over Na_2SO_4. Removal of Et_2O *in vacuo* followed by kugelrohr distillation afforded pale yellow solid as product (90.27 g, 90.3%). TLC R_f 0.41 (DCM); ^1H NMR (400 MHz, $CDCl_3$) δ 7.90 (dd, *J* = 8.2, 1.3 Hz, 1H), 7.84 (dd, *J* = 7.9, 1.4 Hz, 1H), 7.65 (td, *J* = 7.9, 1.3 Hz, 1H), 7.46 – 7.39 (m, 1H), 5.42 (q, *J* = 6.3 Hz,

1H), 2.43 (s, 1H), 1.57 (d, *J* = 6.4 Hz, 3H); ^{13}C NMR (101 MHz, $CDCl_3$) δ 147.80, 140.87, 133.62, 128.11, 127.55, 124.30, 65.55, 24.17; HRMS (CI): Exact mass calcd for $C_8H_9NO_3$ $[M]^-$: 167.0582. Found: 167.0583; HRMS (CI): Exact mass calcd for $C_8H_8NO_2$ $[M+H-H_2O]^+$: 150.05495. Found: 150.05506.

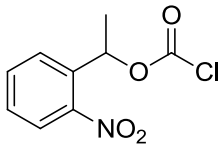

1-(2-nitrophenyl)ethyl chloroformate

To a cooled (0 °C) solution of 2-nitrophenyl ethanol (0.858 g, 5.13 mmol) in dry THF (25 mL) was rapidly added 15% (w/w) phosgene in toluene (10.26 mL, 15.39 mmol) in one portion. The reaction was then allowed to warm to RT and stirred for 36 hours (TLC). After completion of the reaction, the solvents were removed *in vacuo* and gave the product as a light green oil which was used without further purification. TLC R_f 0.68 (30% EtOAc/Hexanes); ^{1}H NMR (400 MHz, $CDCl_3$) δ 8.04 (d, *J* = 8.0 Hz, 1H), 7.77 – 7.66 (m, 2H), 7.52 (t, *J* = 6.8 Hz, 1H), 6.46 (q, *J* = 6.2 Hz, 1H), 1.77 (d, *J* = 6.4 Hz, 3H).

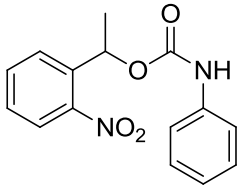

1-(2-nitrophenyl)ethyl phenylcarbamate

To a cooled (0 °C) solution of 1-(2-nitrophenyl)ethyl chloroformate (8.97 mmol) in dry THF (20 mL) and dry toluene (20 mL) was added aniline (1.64 mL, 17.94 mmol) dropwise over 2 minutes. After stirring for 10 minutes at 0 °C, triethylamine (3.00 mL, 21.53 mmol) was added dropwise over 2 minutes. The reaction was then allowed to warm to RT and stirred for 22 hours (TLC). The reaction was concentrated *in vacuo* and the residue was resuspended in 125 mL of Et_2O. The solution was washed twice with NH_4Cl then water and rinsed with brine. Removal of Et_2O *in vacuo* followed by flash column chromatography (DCM) afforded pale yellow oil as product (2.24 g, 87.2%). TLC R_f 0.68 (DCM), 0.50 (30% EtOAc/Hexanes); ^{1}H NMR (400 MHz, $CDCl_3$) δ 7.95 (d, *J* = 8.2 Hz, 1H), 7.75 – 7.56 (m, 2H), 7.42 (t, *J* = 6.9 Hz, 1H), 7.33 (d, *J* = 8.1 Hz, 2H),

7.31 – 7.24 (m, 2H), 7.05 (t, *J* = 7.3 Hz, 1H), 6.72 (s, 1H), 6.37 (q, *J* = 6.5 Hz, 1H), 1.69 (d, *J* = 6.5 Hz, 3H); ^{13}C NMR (101 MHz, $CDCl_3$) δ 152.20, 147.55, 138.30, 137.48, 133.63, 129.05, 128.35, 127.02, 124.53, 123.63, 118.57, 69.12, 22.21; HRMS (ESI): Exact mass calcd for $C_{15}H_{15}N_2NaO_4$ $[M+Na]^+$: 309.08458. Found: 309.08458.

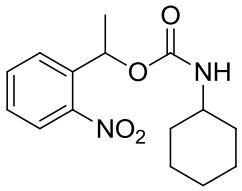

1-(2-nitrophenyl)ethyl cyclohexylcarbamate

To a solution of 2-nitrophenyl ethanol (5.00 g, 29.9 mmol) in dry toluene (140 mL) was added cyclohexyl isocyanate (4.20 mL, 32.9 mmol). The reaction mixture was stirred at 115 °C under reflux for 48 hours. Afterwards, toluene was removed *in vacuo* and the residue was resuspended in 250 mL of Et_2O. The solution was washed twice with water, rinsed with brine, and dried over Na_2SO_4. Removal of Et_2O *in vacuo* followed by flash column chromatography (EtOAc/Hexanes) afforded pale yellow oil as product (6.28 g, 71.9%). TLC R_f 0.51 (30% EtOAc/Hexanes); ^{1}H NMR (400 MHz, $CDCl_3$) δ 7.91 (d, *J* = 8.1 Hz, 2H), 7.70 – 7.57 (m, 4H), 7.45 – 7.36 (m, 2H), 6.23 (q, *J* = 6.3 Hz, 2H), 4.86 (d, *J* = 7.5 Hz, 2H), 3.58 – 3.22 (m, 2H), 2.05 – 0.98 (m, 27H); ^{13}C NMR (101 MHz, $CDCl_3$) δ 154.50, 147.52, 138.92, 133.51, 128.05, 127.09, 124.25, 68.19, 49.85, 33.26, 25.38, 24.77, 22.24; HRMS (ESI): Exact mass calcd for $C_{15}H_{21}N_2NaO_4$ $[M+Na]^+$: 315.13153. Found: 315.13150.

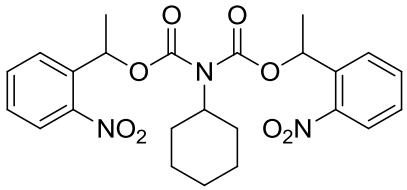

Bis(1-(2-nitrophenyl)ethylcarboxy)cyclohexylamine

To a solution of 2-nitrophenyl ethanol (3.34 g, 20.0 mmol) and finely crushed 5 Å molecular sieves (15 g) in dry toluene (15 mL) was added titanium tetrachloride (1.00 mL of a 1M in toluene, 1.00 mmol). The reaction was stirred at RT for 15 minutes and bis(ethylcarboxy)cyclohexylamine (486 mg, 2 mmol) was added. After stirring at RT for 24 hours, the crude reaction mixture was filtered and the residue washed with toluene. The filtrate

was concentrated *in vacuo* and purified by flash column chromatography (DCM then EtOAc/Hexanes) to afford white powder as product (0.284 g, 29.2%). TLC R_f 0.43 (20% EtOAc/Hexanes); ^{1}H NMR (400 MHz, $CDCl_3$) δ 8.01 – 7.92 (m, 2H), 7.72 – 7.57 (m, 4H), 7.50 – 7.38 (m, 2H), 6.37 (dq, *J* = 10.5, 6.5 Hz, 2H), 4.05 – 3.93 (m, 1H), 1.93 – 1.49 (m, 13H), 1.30 – 0.96 (m, 3H); HRMS (ESI): Exact mass calcd for $C_{24}H_{27}N_3NaO_8$ $[M+Na]^+$: 508.16904. Found: 508.16889.

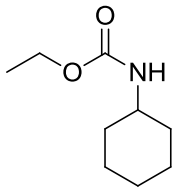

Ethyl cyclohexylcarbamate

To a cooled (-78 °C) solution of cyclohexylamine (13.76 mL, 120 mmol) and triethylamine (33.47 mL, 240 mmol) in dry THF (105 mL) was added dropwise ethyl chloroformate (9.52 mL, 100 mmol). The reaction was allowed to warm to RT and stirred for 20 hours (GC-FID). The crude reaction mixture was filtered, the residue was washed with Et_2O. The filtrate was concentrated *in vacuo* and resuspended with 250 mL Et_2O and 100 mL EtOAc. The solution was washed with saturated NH_4Cl, water, and dried over Na_2SO_4. Removal of the solvent *in vacuo* afforded white solid as product (10.42 g, 62.7%). ^{1}H NMR (400 MHz, $CDCl_3$) δ 4.55 (s, 1H), 4.11 (td, *J* = 13.9, 6.9 Hz, 2H), 3.47 (s, 1H), 2.04 – 1.50 (m, 6H), 1.44 – 1.00 (m, 7H).

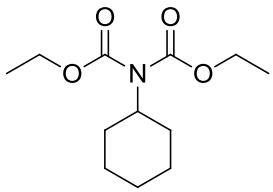

Bis(ethylcarboxy)cyclohexylamine

To a cooled (-78 °C) solution of ethyl cyclohexylcarbamate (10.4 g, 60.7 mmol) in dry THF (210 mL) was added dropwise *n*- butyllithium (24.5 mL of a 2.5 M in hexanes, 61.3 mmol) over 7 minutes. The reaction was stirred for 3 minutes at -78 °C and ethyl chloroformate (6.60 mL, 69.3 mmol) was added over 2 minutes. The reaction was allowed to warm to RT and stirred for 1 hour. The solution was concentrated *in vacuo* and distilled under reduced pressure to afford clear oil (13.30 g, 90.1%).^{1}H NMR (400 MHz, $CDCl_3$) δ 4.20 (q, *J* = 7.1 Hz, 4H), 4.01 (ddt, *J* = 15.7,

11.9, 3.7 Hz, 1H), 1.92 – 1.52 (m, 7H), 1.35 – 1.18 (m, 8H), 1.15 – 0.99 (m, 1H). ^{13}C NMR (101 MHz, $CDCl_3$) δ 154.32, 62.64, 57.62, 30.26, 26.22, 25.29, 14.10.